

AN EFFICIENT MODELING PROCEDURE FOR SIMULATION OF DYNAMICS OF ADHESIVELY BONDED JOINTS

Anindya Deb¹, Indrajit Malvade^{1*}

¹CPDM, Indian Institute of Science, Bangalore, India

* Currently with John Deere Technology Center - India, Pune, India

ABSTRACT

The present study is aimed at developing a new computationally efficient modeling procedure that predicts well the nonlinear mechanical behavior of adhesively bonded joints. The approach is thought to be particularly beneficial for computationally intensive vehicle crash simulations. Two other conventional modeling approaches are considered, that is, accounting for adhesive layer between shell-based substrates/flanges with monolithic solid elements, and defining a tied contact with failure condition in lieu of the solid elements. The approach presented here and not previously reported in the literature is an enhancement of the latter technique with equivalent properties being assigned to the substrates in the overlap segment of a joint model. A semi-analytical procedure is outlined in detail for arriving at the equivalent properties of substrates by accounting for shear properties of an epoxy adhesive which is geometrically not represented in the model. It is shown that the effect of strain rate on adhesive behavior can be elegantly incorporated in the proposed equivalent property-based approach via Material Type 24 in LS-DYNA for intended applications of dynamics such as vehicle crash safety assessment. The computational efficiency and accuracy of the present approach are established by comparing results yielded by it against experimental data and detailed shell-solid modeling technique.

INTRODUCTION

To develop vehicles with BIW structures deploying adhesively bonded joints, it would be necessary to carry out efficient finite element modeling of the joints. Adhesive in joints are commonly modeled as springs, but this is an ad-hoc and inconvenient modeling procedure as spring properties are not intrinsic in nature and are not mesh size-independent [1, 2]. Modeling of adhesive with solid elements can provide good prediction of mechanical behavior of adhesively bonded joints, however, usage of minute solid elements in a large vehicle model can render analysis turn-around time nearly impracticable especially for compute-intensive nonlinear contact-impact problems [3]. CONTACT_TIEBREAK_{X} (where, X = SURFACE_TO_SURFACE) condition in LS-DYNA can be used for modeling adhesively bonded joints in large models, but this approach may give rise to a stiffer joint response as shown in the current investigation and does not have the provision for specifying the dependence of adhesive properties on strain rate or temperature [4].

Attempts have been made to develop simplified finite element models for adhesively bonded joints. Various simplified joint modeling techniques [3] to predict the stiffness of lap shear joints are available but the studies are limited to elastic range and do not include, for example, the effects of strain rate and temperature. Alcan's joint-line element [5] can be used to minimize the details required to model joints in a full vehicle model. However, this approach requires a large database. Beevers [6] developed an undercut element concept using solid elements for representing adhesive for obtaining stiffness of coach (T-peel) joints, but the study was based on linear elastic models and applied only to coach joints.

The objective of the current work is to minimize the details required to model adhesively bonded joints in vehicle structures for computationally demanding nonlinear applications such as crash analysis. Although stresses in adhesive cannot be obtained from the approach to be discussed here, it can yield accurate predictions of overall joint stiffness, resultant force in a joint, and the elongation of the joint in completely elastic phase or after onset of plasticity in one or more of the joint constituents.

CONTACT MODELING OF ADHESIVE IN A BONDED JOINT

A geometrically accurate representation of localized adhesive in a joint would be to model the same with solid elements while substrates, normally being thin flat or curved plates, can be modeled with shell elements [7]. It has been shown that this shell-solid representation can yield good predictions of double lap shear (DLS) joint behavior [7] in terms of force-displacement histories at various loading rates and temperatures. However, usage of minute solid elements in a large vehicle model would make crash analysis impracticable in terms of analysis turn-around time. Therefore, a more efficient modeling method would be to replace adhesive in a joint by the CONTACT_TIEBREAK_{X} (where, X = SURFACE_TO_SURFACE) condition in LS-DYNA. This is similar to what is described as ‘cohesive zone modeling’ by some investigators in the published literature. Here, the approach of representing bonding between substrates until failure using a suitable contact interface in LS-DYNA as mentioned above is termed simply as ‘contact modeling’. In the present study, the utility of this procedure is advanced further by deriving equivalent fictitious properties for the substrates in the joint region. By comparing with test results obtained for a DLS joint with DP (dual phase) steel substrates and an epoxy adhesive, it is shown that the suggested strategy of using equivalent properties representing the combined behavior of metallic substrates and structural adhesive yields superior correlation than the conventional approach in which the actual properties of steel would be assigned to the substrates. The conventional and equivalent property-based methods are described in the ensuing sections.

Conventional Approach

The contact condition defined by the keywords CONTACT_TIEBREAK_{X} (where, X = SURFACE_TO_SURFACE) in LS-DYNA has been recommended for representing adhesives [3]. The tiebreak contact allows separation of tied surfaces using the following failure criterion:

$$\left(\frac{|\sigma_n|}{NFLS} \right)^2 + \left(\frac{|\sigma_s|}{SFLS} \right)^2 \geq 1, \quad (1)$$

where NFLS is the normal failure stress and SFLS is the shear failure stress. The DLS joint modeled using the above contact condition is shown in Fig. 1. It is seen that the adhesive is not represented with physical elements, instead the integrity of the joint is simulated by defining the CONTACT_TIEBREAK_{X} condition between the substrates in the joint overlap region.

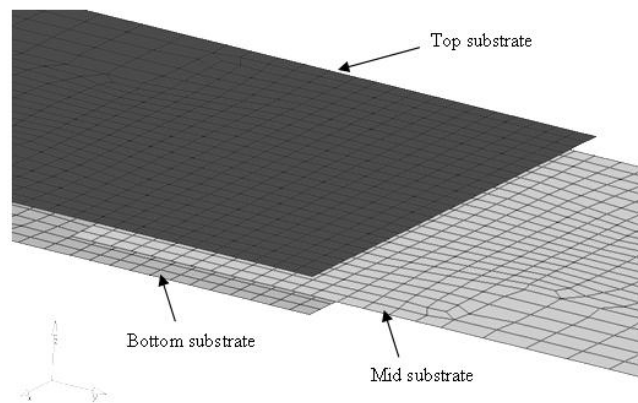


Fig. 1. Contact model for a DLS joint (substrates are shown truncated)

It is noted that elasto-plastic material behavior is assumed for the DP steel substrates defined through Von Mises yield condition combined with isotropic hardening. The stress-strain behaviors of DP steel and adhesive obtained from tensile coupon tests are given in Figs. 2 and 3 respectively. Electronic extensometer was employed in these tests to accurately measure strain in the longitudinal direction. It can be seen from the figures mentioned that adhesive is markedly sensitive to strain rate even at low values of the same (test loading rates of 1 mm/min, 100 mm/min and 500 mm/min corresponded to strain rates of 0.0002 s^{-1} , 0.019 s^{-1} and 0.09 s^{-1} respectively) while the response of DP steel is marginally dependent on test loading rate. The relevant material properties for simulation were extracted from the stress-strain curves presented and Poisson's ratios were also obtained with the help of lateral strain gages fixed to selected coupon specimens. As the shear strength of adhesive was not directly measured, an estimate of the shear strength was obtained separately through numerical simulation using Exponential Drucker Prager (EDP) and Von Mises (VM) constitutive models [8]. A finite element model replicating pure shear condition is shown in Fig. 4. The variations of shear stress with respect to shear strain for EDP and VM yield criteria are shown in Fig. 5 for different loading rates at room temperature. The normal failure stress of adhesive, NFLS in Eqn. (1), can be obtained from one of the curves in Fig. 3, while the shear failure stress, SFLS in Eqn. (1), can be estimated using the information given in Fig. 5.

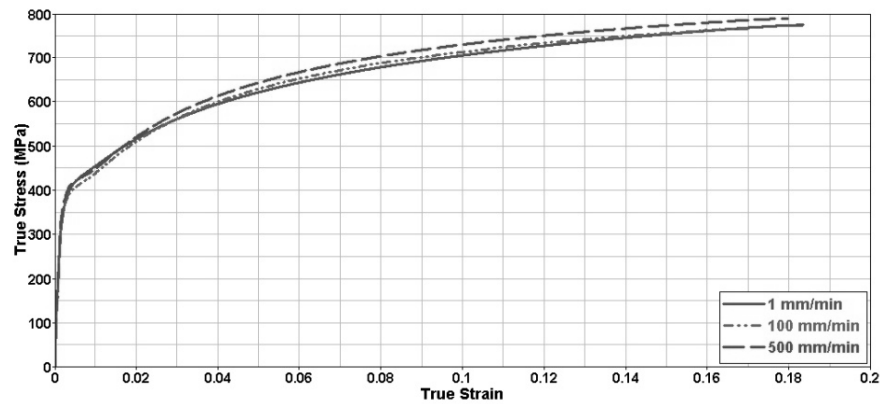


Fig. 2. Stress-strain characteristics of DP steel at room temperature

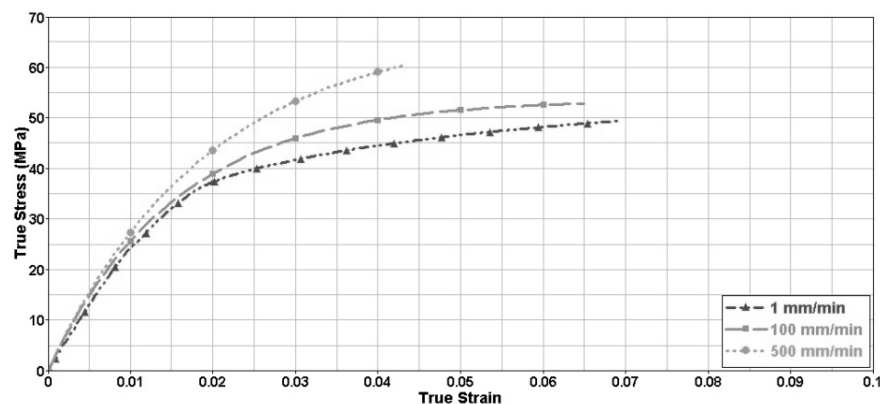


Fig. 3. Stress-strain characteristics of adhesive at room temperature

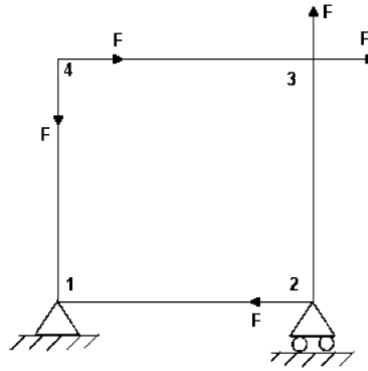


Fig. 4. Boundary and loading conditions with one shell element for simulation of a pure shear test

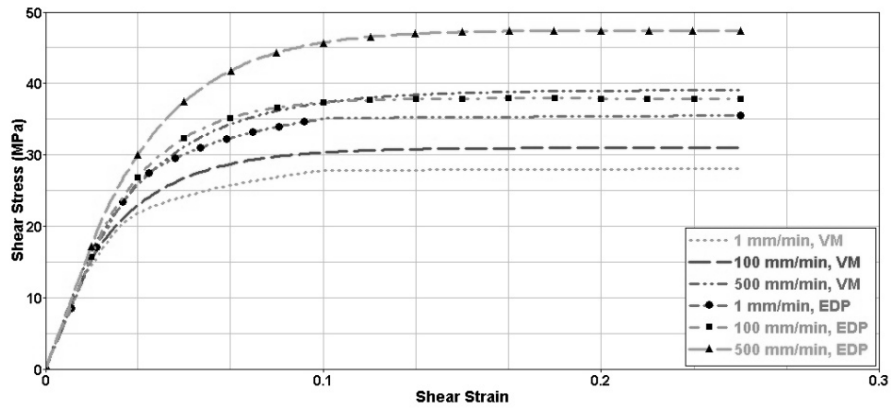


Fig. 5. Derived shear stress-strain characteristics of adhesive using EDP and VM yield criteria

New Equivalent Property-Based Approach

The procedure outlined above relies on using actual properties of the substrates in the joint overlap region, however, as will be seen later, this leads to a stiffer prediction of joint behavior. An alternative methodology suggested here is to model the overlap region, as depicted in Fig. 6, of an adhesively-bonded DLS joint with equivalent fictitious properties combined with the CONTACT_TIEBREAK_{X} condition already discussed. In contrast, a more detailed representation of the same joint under applied in-plane loading is shown in Fig. 7.

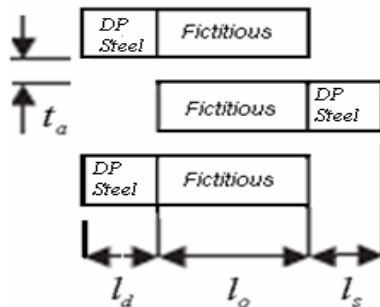


Fig. 6. Longitudinal section of equivalent joint model concept through the gage length

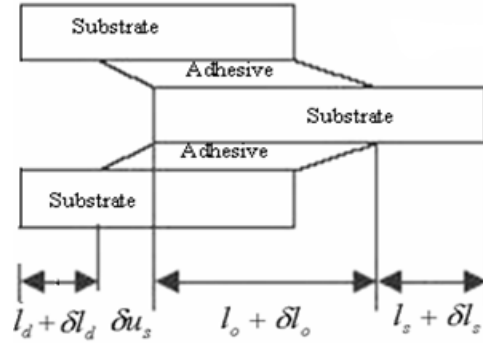


Fig. 7. Kinematics of deformation in a longitudinal section through the gage length of a DLS specimen

The stress-strain characteristic of the equivalent material is derived by assuming that the force-extension joint curve yielded by the equivalent joint properties will match the force-extension response with adhesive being actually present between pairs of substrates; the stated criterion for equivalence is applied to simplified representations of the DLS joint in which stress in each joint component (i.e. substrate or adhesive layer) is assumed as constant spatially. It needs to be mentioned that in the simplified models with fictitious and actual materials in the overlap region as given in Figs. 6 and 7 respectively, only the gage length used by extensometer in DLS joint tests is considered.

It is assumed that the overall extension of the DLS joint shown as deformed in Fig. 7 is an aggregate of the deformations of the following segments of the joint due to a load increment δF : (i) single leg of initial length l_s , (ii) double leg of initial length l_d , and (iii) overlap of initial length l_o . The substrate is of width b , thickness t , and Young's modulus E . The adhesive has a thickness t_a , and shear modulus G_a . The overall length of the lap joint assumed in this analysis is equal to the gauge length (i.e. 25 mm) of the extensometer used to measure the experimental joint extensions; thus $l_o = 12\text{ mm}$ and $l_d = l_s = 6.5\text{ mm}$. The deformed shape of the joint due to tensile loading is shown in Fig. 7.

An incremental procedure is followed in predicting the joint force-extension behavior. The history of joint force-extension is traced by applying equal incremental load steps (δF) and computing corresponding displacement increments (δu_i). For each load step, deformation of each segment of the joint is calculated based on the material properties corresponding to the current state of stress in the respective segment. The total incremental joint deformation is obtained by summing up the deformations of the relevant segments. The total load is the cumulative sum of all load steps including the current one; similarly, the total displacement is the cumulative sum of all incremental joint deformations of the current and previous load steps. The estimations of the extensions, assuming uniform stress in any relevant segment, are now discussed below:

(i) Extension in single leg segment:

The single leg segment supports the total joint force F . Due to an incremental joint load δF , the change in axial displacement of the single leg in the linear elastic region of the stress-strain curve of DP steel can be expressed as

$$\delta l_{si} = \delta \epsilon_{ei} l_{si} = \frac{\delta \sigma_s}{E} l_{si} = \frac{(\delta F) l_{si}}{btE}. \quad (2)$$

It may be noted that the letter i appearing in any subscript in Eqn. (2) implies the value of the associated quantity at the time of applying the i^{th} load increment; for example, l_{si} is the value of the non-overlap length l_s of the single leg segment in Fig. 7 when the i^{th} load increment is applied. This notation is followed henceforth for all simplified joint parameters.

The change in axial displacement in the plastic regime ($\sigma_s > \sigma_{yield}^{DPSteel}$) for the present segment can be estimated as

$$\delta l_{si} = \delta \varepsilon_{pi} l_{si} = \frac{\delta \sigma_s}{E_{Ti}} l_{si} = \frac{(\delta F) l_{si}}{btE_{Ti}}. \quad (3)$$

where, the tangent modulus E_{Ti} can be obtained from the relevant stress-strain curve of DP steel as

$$E_{Ti} = \frac{\sigma_{i+1} - \sigma_{i-1}}{\varepsilon_{i+1} - \varepsilon_{i-1}}. \quad (4)$$

(ii) Extension in double leg segment:

Each substrate in the double leg segment bears half of the incremental joint force δF . The incremental elastic and plastic displacements in this segment can be obtained as given below:

In the elastic condition,

$$\delta l_{di} = \delta \varepsilon_{ei} l_{di} = \frac{\delta \sigma_d}{E} l_{di} = \frac{(\delta F) l_{di}}{2btE}. \quad (5)$$

In the plastic region of stress-strain behavior,

$$\delta l_{di} = \delta \varepsilon_{pi} l_{di} = \frac{\delta \sigma_d}{E_{Ti}} l_{di} = \frac{(\delta F) l_{di}}{2btE_{Ti}}. \quad (6)$$

(iii) Extension in overlap segment:

The axial displacement of the overlap segment consists of tensile deformation of the central substrate and shear deformation of the adhesive layers as shown in Fig. 7. The tensile deformation in the top and bottom substrates in the overlap region does not probably contribute to any resultant deformation in the overlap segment.

In the overlap portion of the central substrate, the tensile stress is maximum at the loaded end and zero at the free end. Hence, it can be assumed to be subject to an average force of $F/2$. The elastic or plastic displacement increment in the central substrate will then be given by a relation similar to Eqn. (5) or (6) with the replacement of the parameter l_{di} by l_{oi} as given below in Eqns. (7) and (8):

In the elastic condition,

$$\delta l_{oi} = \delta \varepsilon_{ei} l_{oi} = \frac{\delta \sigma_o}{E} l_{oi} = \frac{(\delta F) l_{oi}}{2btE}. \quad (7)$$

And, in the plastic condition,

$$\delta l_{oi} = \delta \varepsilon_{pi} l_{oi} = \frac{\delta \sigma_o}{E_{Ti}} l_{oi} = \frac{(\delta F) l_{oi}}{2btE_{Ti}}. \quad (8)$$

The adhesive layers are subject to shear stresses at their interfaces with the substrates. The shear stress in each adhesive layer is due to half the incremental load δF carried by it. Thus, the change in axial displacement of the joint due to shear deformation of the adhesive layers would be:

In the elastic condition,

$$\delta u_{si} = \delta \gamma_{ei} t_a = \frac{\delta \tau_a}{G_a} t_a = \frac{(\delta F) t_a}{2bl_{oi} G_a}. \quad (9)$$

And, in the plastic condition,

$$\delta u_{si} = \delta \gamma_{pi} t_a = \frac{\delta \tau_a}{G_{aTi}} t_a = \frac{(\delta F) t_a}{2bl_{oi} G_{aTi}}, \quad (10)$$

where, G_{aTi} is the tangent shear modulus of adhesive at the i^{th} increment of load that can be estimated from the shear stress-strain curve of adhesive in a manner similar to the estimation of E_{Ti} for DP steel given by Eqn. (4).

The total change in axial displacement of the DLS joint is then a summation of Eqns. (3) or (4), (5) or (6), (7) or (8), and (9) or (10), i.e.,

$$\delta u_i = \delta l_{si} + \delta l_{di} + \delta l_{oi} + \delta u_{si}, \quad (11)$$

where, it can be said that

$$\delta u_i = \left(\frac{l_{si}}{btE^*} + \frac{l_{di}}{2btE^*} + \frac{t_a}{2bl_{oi} G_a^*} + \frac{l_{oi}}{2btE^*} \right) \delta F. \quad (12)$$

The material parameters with asterisk in Eqn. (12) can be elastic or tangent moduli (i.e. $E^* = E$ or E_{Ti} ; $G_a^* = G_a$ or G_{Ti}) according as the relevant segment is in elastic or plastic condition.

Thus, the total joint axial displacement at the end of i^{th} load increment can be expressed as

$$u_i = u_{i-1} + \delta u_i. \quad (13)$$

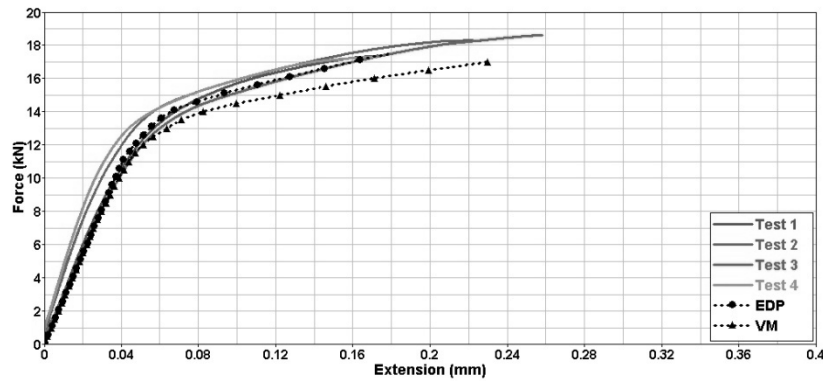


Fig. 8. Comparison of predicted behaviors with test results at room temperature with 1 mm/min rate

Prediction of force-displacement response for a DLS joint using Eqn. (12) was implemented in a computer program. The predicted responses using VM and EDP yield criteria are compared in Fig. 8 with results of tensile tests carried out at a cross-head speed of 1 mm/min on four similar DLS joint specimens. The test results were found to be consistent across the four samples. The computed force-displacement behavior arising from the EDP criterion appears to tally better with experimental results than the prediction yielded by the VM criterion.

A similar procedure as enumerated above can be followed in obtaining the incremental displacement for the simplified joint concept of Fig. 6 in which adhesive is to be replaced by assigning equivalent material properties to the substrates in the joint overlap region. The steps involved leading to the expression of incremental displacement for a given incremental applied force in the middle substrate are described below:

In the overlap portion of the middle substrate in Fig. 6, the tensile stress is maximum at the loaded end and zero at the free end. Hence, it can be assumed to be subject to half of the applied incremental load δF . The incremental displacement due to this load in the middle substrate in the overlap region is then

$\frac{(\delta F)l_{oi}}{2btE_{eq}^*}$, assuming that E_{eq}^* is the equivalent elastic or tangent modulus of the fictitious material in the

substrate. As in the case of substrates with adhesive in Fig. 7, it is assumed that, due to the presence of contact interface between the substrates, the overlap parts of the outer substrates do not contribute any additional displacement to the joint. In the non-overlap region of the middle substrate, the entire

incremental force δF can be assumed to act resulting in an incremental displacement of $\frac{(\delta F)l_{si}}{btE^*}$. Each of

the non-overlap regions of the outer substrates is subject to half the incremental load δF and therefore an

incremental displacement of $\frac{(\delta F)l_{di}}{2btE^*}$. The total incremental displacement in the equivalent model for the

i^{th} load increment can then be written as:

$$(\delta u_i)_{eq} = \left(\frac{l_{oi}}{2btE_{eq}^*} + \frac{l_{si}}{btE^*} + \frac{l_{di}}{2btE^*} \right) \delta F. \quad (14)$$

For the fictitious material-based model to be equivalent to the actual joint, the displacement increments given by Eqns. (14) and (12) should be equal. Thus, equating the right sides of Eqns. (12) and (14), the following relation for equivalent stiffness (elastic or tangent) is obtained:

$$E_{eq}^* = \frac{l_{oi}^2 E^* G_a^*}{tt_a E^* + l_{oi}^2 G_a^*}. \quad (15)$$

It needs to be mentioned that the modulus E^* corresponds to the state in the overlap region of the middle substrate at the time of application of i^{th} load increment. An incremental procedure is now followed to obtain stress-strain behavior of the fictitious material in the overlap segment as per Eqn. (15). It is evident from Eqn. (15) that the derivation of the stress-strain behavior of the equivalent joint requires, in addition to the tensile stress-strain data of substrate steel, the shear stress-strain data of adhesive. The shear stress-strain data can either be obtained experimentally or estimated numerically using the VM or EDP criterion as shown in Fig. 5.

Following an incremental procedure as described earlier using Eqns. (2) through (10) which will yield the values of E^* and G_a^* on the right side of Eqn. (15), the value of E_{eq}^* can be determined. The equivalent tensile stress-strain curves generated in this manner for the fictitious joint overlap material for both VM and EDP yield criteria (which affect the values of G_a^*) are given in Fig. 9 for various loading rates (and consequently, strain rates) at room temperature. It is noted that for a given strain rate, only one of the two corresponding curves in Fig. 9 based on VM and EDP criteria can be used for simulating joint behavior using the equivalent property approach.

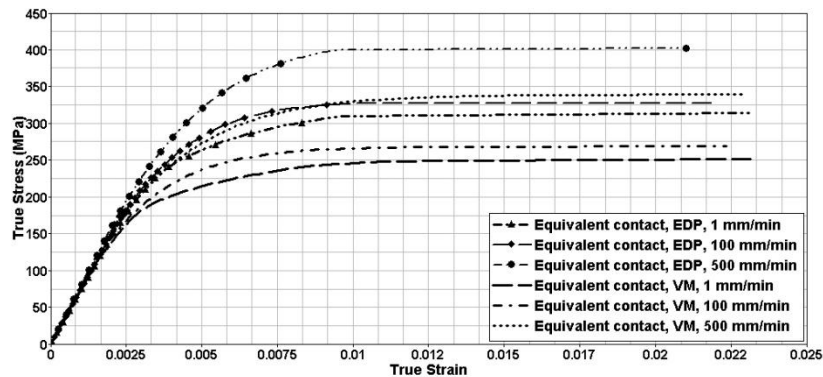


Fig. 9. Equivalent stress-strain curves for fictitious joint overlap material with contact interface

SIMULATION RESULTS FOR CONVENTIONAL AND EQUIVALENT PROPERTY-BASED CONTACT APPROACHES

Using the conventional representation of adhesive using a contact interface as described in a previous section, a finite element analysis (with shell elements only) of the DLS joint under consideration has been carried out and the computed force-displacement curve is compared in Fig. 10 with the test results for similar specimens at room temperature and a loading rate of 1 mm/min. As expected, the simulation yields a stiffer response as the adhesive is not physically modeled and only its failure under a combination of normal and shear stresses is accounted for.

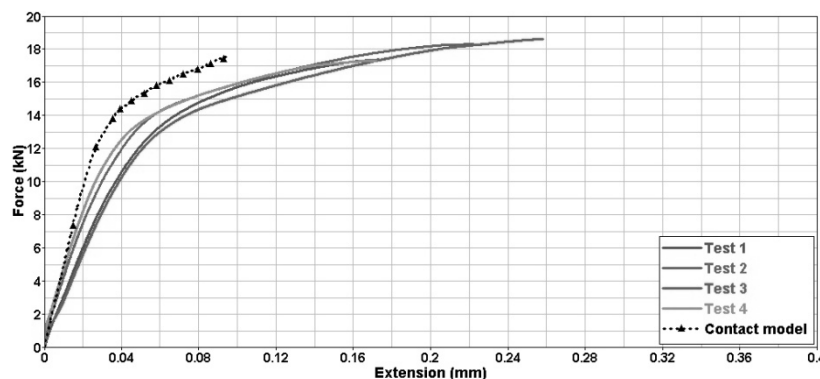


Fig. 10. Comparison of simulation result using conventional contact model with test results at 1 mm/min

Next, equivalent properties are assigned to the substrates in the overlap region shown with dark shade in the finite element model of current DLS in Fig. 11. As in the previous case, with ease of modeling and integrity of the joint in mind, and to simulate failure of adhesive, the CONTACT_TIEBREAK_{X}

(where, X = SURFACE_TO_SURFACE) interface is again defined between the substrates and analysis is carried out using the explicit LS-DYNA code.

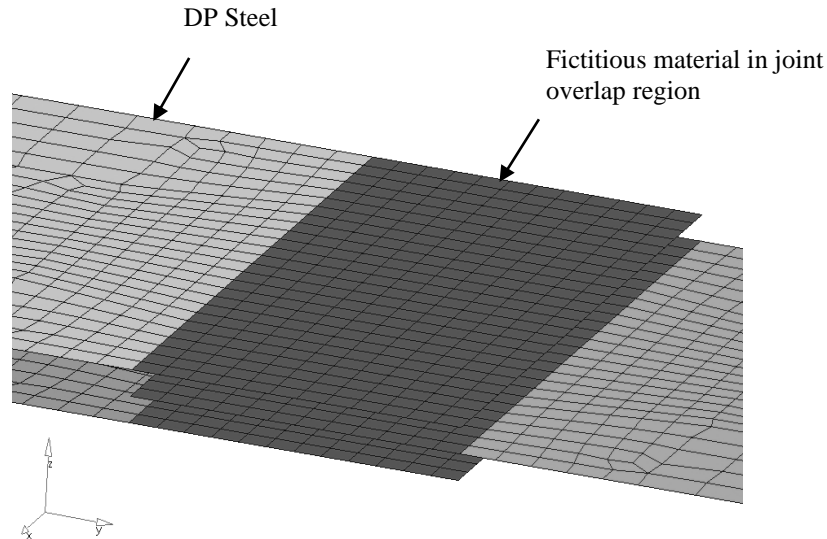


Fig. 11. Equivalent property-based DLS joint finite element model

For the case in which the EDP-based equivalent stress-strain curve of Fig. 9 at 1 mm/min is assigned to the fictitious material in the substrates through Material Type 24 in LS-DYNA, the resulting joint response is shown in Fig. 12 along with corresponding test-based and detailed shell-solid model-based force-extension curves [7]. It is seen in Fig. 12 that the present computed response is somewhat stiffer in the plastic region compared to the average experimental behavior and numerical data from the detailed model shown in Fig. 13 [7] in which adhesive was represented with solid elements. The analysis is repeated by assigning the VM-based equivalent stress-strain curve of Fig. 9 at 1 mm/min to the overlap region in the substrates and the resulting force-extension behavior is presented in Fig. 14. In the latter figure, extremely good correlation is observed between the current numerical prediction and previous test and simulation results. It can therefore be concluded, based on Figs. 12 and 14, that the VM-based equivalent stress-strain behavior at a strain rate corresponding to a loading rate of 1 mm/min can be preferred over the EDP-based equivalent stress-strain behavior for obtaining a force-displacement prediction of the joint that tallies well with experimental results.

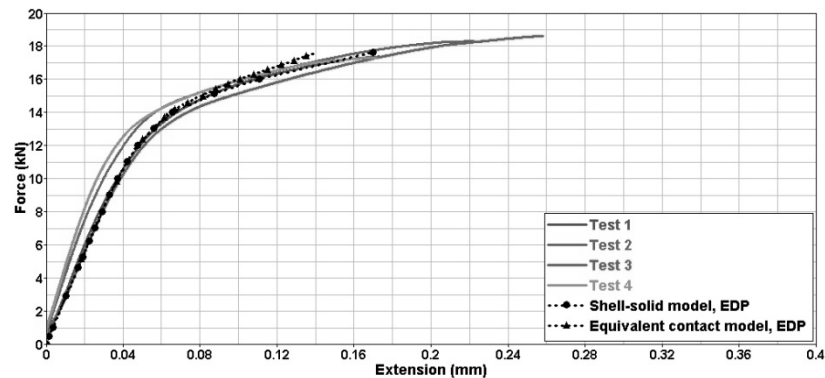


Fig. 12. A comparison of results from the equivalent property (EDP)-based contact finite element model, detailed FEA [7] and tests performed at room temperature at 1 mm/min

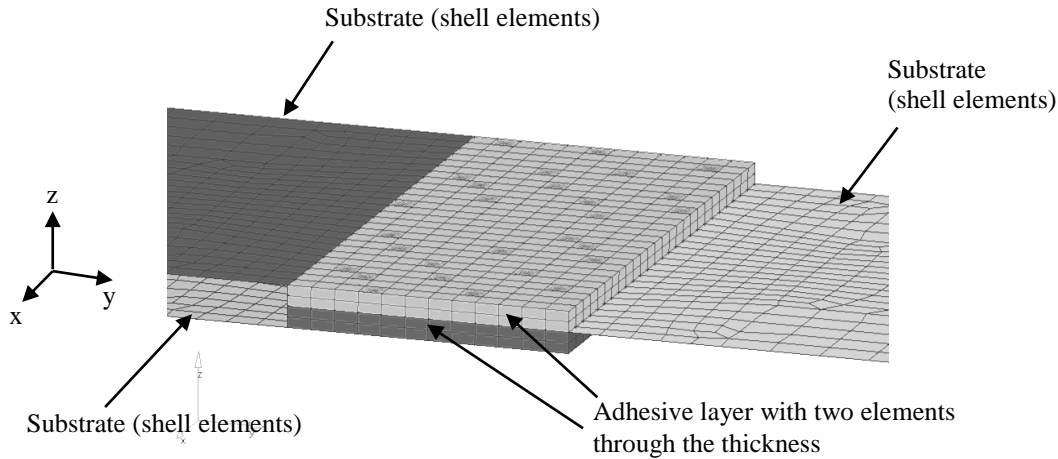


Fig. 13. Shell-solid finite element model of DLS joint with two elements through the thickness of each adhesive layer (substrates are shown truncated for a closer view of joint overlap region) [7]

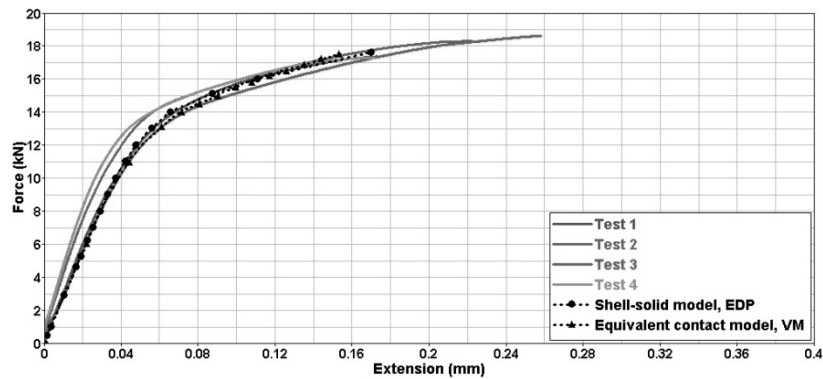


Fig. 14. A comparison of results from the equivalent property (VM)-based contact finite element model, detailed FEA [7] and tests performed at room temperature at 1 mm/min

Table 1. A comparison of total run times for various finite element models for a given maximum joint displacement using explicit LS-DYNA solver

Model configuration	Simulation run time (minutes)	Total number of elements in the model
Shell-solid	9	4458
Equivalent property (VM) with contact (refined)	7	3210
Equivalent property (VM) with contact (coarse)	3	1832

With the accuracy of the current equivalent property (VM)-based approach established, a comparison is given in Table 1 of simulation run times for the detailed shell-solid model and two meshing configurations, i.e. fine and coarse, for the shell-only model employing the equivalent properties in

substrates in the joint overlap region. The equivalent property-based models, especially the coarse variety with mesh biasing, are observed to be substantially efficient computationally with respect to the detailed model which is generally preferred in linear elastic analysis but may be unsuitable for nonlinear dynamic problems such as crashworthiness evaluation of automotive body structures.

RATE DEPENDENT MODELING OF DLS JOINT USING EQUIVALENT PROPERTY (VM)-BASED CONTACT FINITE ELEMENT MODEL

The behavior of polymeric adhesive, as is clear from Fig. 3, is strain rate-dependent. In impact-related problems, the strain rate will not only vary with time at a given geometrical point but also spatially at an instant of time. There is thus a need to capture the dependence of the properties of an adhesively bonded joint on strain rate for problems of dynamics. The present equivalent property (VM)-based approach appears to be ideally suited for this purpose as the effect of strain rate using a look-up table consisting of a series of dynamic yield stress versus effective plastic strain curves for different strain rates as depicted in Fig. 15 [4] can be specified using Material Type 24 in LS-DYNA. Equivalent stress-strain curves (based on adhesive shear properties derived numerically using the VM yield criterion) for 1 mm/min (i.e. 0.0002 sec^{-1}), 100 mm/min (i.e. 0.019 sec^{-1}) and 500 mm/min (i.e. 0.09 sec^{-1}) along with an extrapolated curve for a strain rate of 0.2 sec^{-1} have been used here. It is noted that intermediate values of yield stress are found by interpolating between the given curves; on the other hand, if a value of strain rate happens to be outside the defined range, either the first or the last curve determines the yield stress depending on the proximity of the rate to these curves [4].

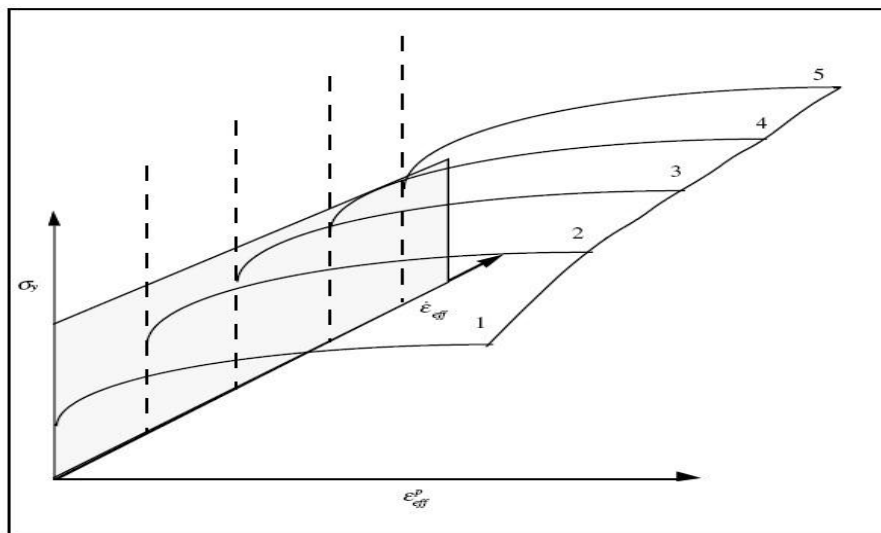


Fig. 15. Rate effects are included by defining hardening curves for a range of strain rates [4]

To validate the tensile response of the rate-dependent model, a four-node single Belytschko-Tsay shell element is used for simulation of pure tension test. The load and boundary conditions applied to the model are shown in Fig. 16. The applied strain rate is controlled by the displacement-time curve defined in the LS-DYNA input file. Since LS-DYNA is an explicit code, designed for solving dynamic problems, attempts to simulate the extremely low strain rate tests were found to have numerical stability problems, and the analyses took an extremely long time to reach the failure strain, even by using only a single element. Additionally, in a realistic problem of impact dynamics (i.e. the intended domain of application), the strain rates are well above the quasi-static level. Therefore, the low strain rate case of 0.0002 sec^{-1} is not considered here. The input and simulated stress-strain curves for the strain rates of 0.019 sec^{-1} and 0.09 sec^{-1} are shown in Fig. 17 and are in extremely good agreement with each other in pairs.

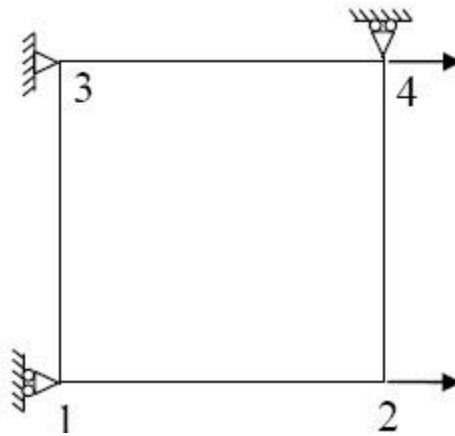


Fig. 16. Boundary and loading conditions for simulation of pure tension test

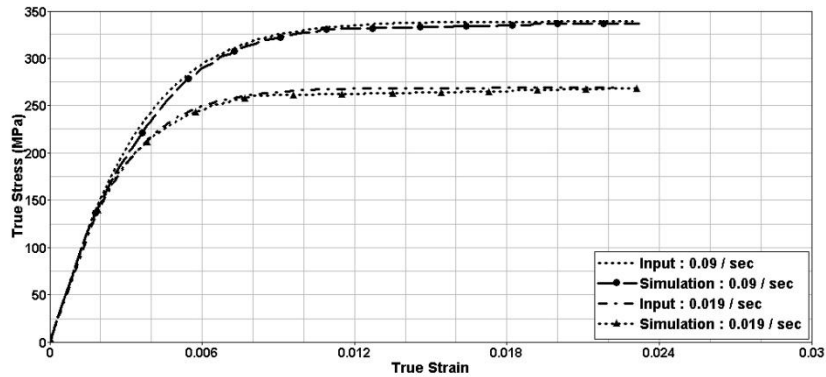


Fig. 17. Validation of tensile responses of the rate-dependent VM material (Type 24) model

With the consistency of the strain rate-dependent modeling approach using Material Type 24 verified, the analysis of DLS joint is carried out with equivalent properties in the overlap region for different strain rates as mentioned earlier. For an applied tensile loading rate of 500 mm/min, the simulation result using the rate-dependent equivalent property (VM)-based model yields quite a satisfactory correlation with test results as shown in Fig. 18.

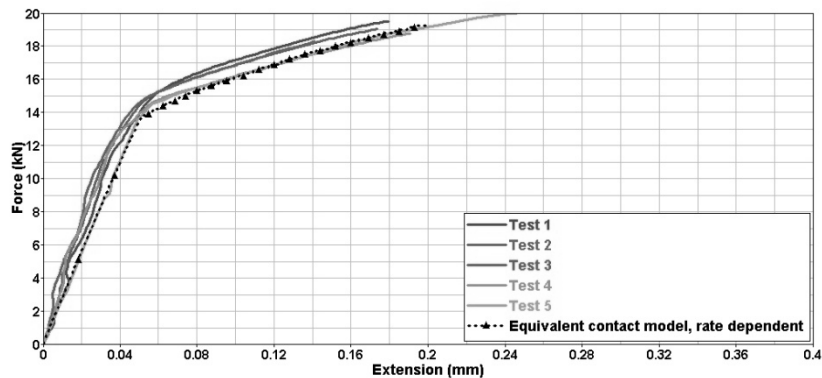


Fig. 18. A comparison of predicted DLS joint behavior at 500 mm/min using rate-dependent equivalent property (VM)-based model and experimental results

CONCLUSIONS

In the current paper, a computationally efficient finite element modeling procedure that predicts well the nonlinear mechanical behavior of adhesively bonded joints has been presented. The proposed method in which equivalent properties are assigned to the substrates in the overlap region of an adhesively bonded joint is shown to be more accurate than an existing ‘cohesive zone’-type modeling procedure in which actual properties of substrates are used and the failure of adhesive is represented by a CONTACT_TIEBREAK_SURFACE_TO_SURFACE interface. It is noted that the latter contact condition is used in the equivalent property-based approach also and substrates are modeled with Belytschko-Tsay shell elements in both methods while adhesive is not geometrically represented in either contact-based method. For assessing accuracy of the current equivalent property-based procedure, earlier results from a detailed shell-solid model of a DLS joint in which adhesive is geometrically modeled with solid elements and monolithically mated with shell elements representing substrates are given along with pertinent experimental data of DLS joints. A semi-analytical procedure is outlined in detail for arriving at the equivalent properties of substrates by accounting for shear properties of an employed epoxy adhesive. It is finally shown that the effect of strain rate on adhesive behavior can be elegantly incorporated in the proposed equivalent property-based approach via Material Type 24 in LS-DYNA for intended applications of dynamics such as supporting vehicle crash safety design.

REFERENCES

- [1] Lu J. P., Newaz G., Gibson R., “Computational simulation of adhesively bonded aluminum hat sections under plastic bucking deformation”, SAE technical series, Paper No. 2001-01-2703.
- [2] Wagner D. A., “FEA (Finite element analysis) modeling for body-in-white adhesives”, SAE Paper No. 960784.
- [3] Xiao X. R., Foss P. H. , Schroeder J. A., “Stiffness prediction of the double lap shear joint. Part2: finite element modeling”, Int J Adhes Adhes 2004; 24: 239–246.
- [4] LS-DYNA Keyword User’s Manual, Volume II (Material Models, References and Appendices), Version 960, Livermore Software Technology Corporation.
- [5] McGregor I. J., Nardini D., Gao Y., Meadows D. J., “The development of a joint design approach for aluminum automotive structures”, SAE Technical Paper Series, 922112, 1992.
- [6] Beevers A., Steidler S. M., Durodola J., Coackley M., “Analysis of stiffness of adhesive joints in car bodies”, J Mater Process Technol 2001; 118: 96 – 101.
- [7] Malvade I., Deb A., Biswas P. and Kumar A., “Numerical prediction of load-displacement behaviors of adhesively bonded joints at different extension rates and temperatures”, Computational Materials Science, 44(4), 1208-1217 (2009).
- [8] Deb A., Malvade I., Biswas, P. and Schroeder, J. T., “An experimental and analytical study of the mechanical behaviour of adhesively bonded joints for variable extension rates and temperatures”, International Journal of Adhesion and Adhesives, 28, 1-15 (2008).